

Design of restrained pneumatic formwork – Inverse form finding and materialisation for free form geometries

Chaoyu DU^{a*}, Ziqi WANG^b, Tom VAN MELE^a, Philippe BLOCK^a

*Block Research Group, ETH Zurich
Stefano-Franscini-Platz 1, 8093, 8049
chaoyu.du@arch.ethz.ch

^a Block Research Group, ETH Zurich, Switzerland
^b CRCL & Sycamore, EPFL, Switzerland

Abstract

This paper presents a method for the inverse design of restrained air-supported structures or pneumatic formwork. The proposed approach consists of two main steps. We first solve a best-fit optimisation using the force-density method. Considering the self-weight and air pressure, the optimisation determines an equilibrium force distribution in the membrane as a discrete network that closely approximates a given input surface. Subsequently, the force density results are materialised. By applying the finite element method, we tailor the material properties of the membrane, specifically adjusting its stiffness, to achieve the desired structural characteristics. To demonstrate the adaptability and effectiveness of our method, the paper concludes with a series of examples showcasing its application.

Keywords: pneumatic structure, force density method, finite element method, form-finding, inverse design

1. Introduction

Inflatable, or pneumatic structures are tensile structures supported by pressurised air. They have gained increasing popularity across a diverse range of applications [1]. Characterised by their lightweight, fast deployment and the capability to cover large spaces, inflatable structures have established their significance beyond temporary shelters or installations, serving as fundamental components in essential architecture such as sports stadiums and exhibition halls [2], [3].

Pneumatic structures are stabilised by air pressure and can naturally form synclastic geometries (Figure 1 left). This property makes them ideal to be used as formwork for domes and self-supporting vaults or shell structures, which are dominated by the synclastic curvature to direct compressive forces towards the supports [4], [5], [6], [7], [8] (Figure 1 right).

Despite their advantages, designing pneumatic formworks for constructing geometrically precise structures, particularly those with free-form shapes, presents substantial challenges. Inflatables, comprising membrane patches, are form-active structures prone to deformation under external loads. Incorporating restraint mechanisms, such as cables or webbing, into the inflatable system can significantly enhance stability and precision [9], [10], [11]. These enhancements allow for the use of a "loose balloon", which does not necessitate precise pre-inflation positioning yet achieves exact geometry upon inflation due to the existence of the restraints. This method shifts the design challenge to determining the optimal constraints under given

loads, requiring an optimisation process to identify the desired force distribution and materialisation of these constraints.

Previous work [12], [13] has investigated the design of cable network constraints. Advancements in digital fabrication technologies, including 3D printing [14] and CNC knitting [15], have enabled the creation of membrane restraint materials with variable stiffness. However, a clear and comprehensive framework for designing these constraint systems for inverse design in architectural applications remains unclear. Thus, the primary aim of this paper is to delineate a detailed workflow for the inverse design of restrained pneumatic formwork with materials that, once fabricated, can be inflated to form a target geometry. Furthermore, this paper proposes methodologies for materialising the restraint mechanism.

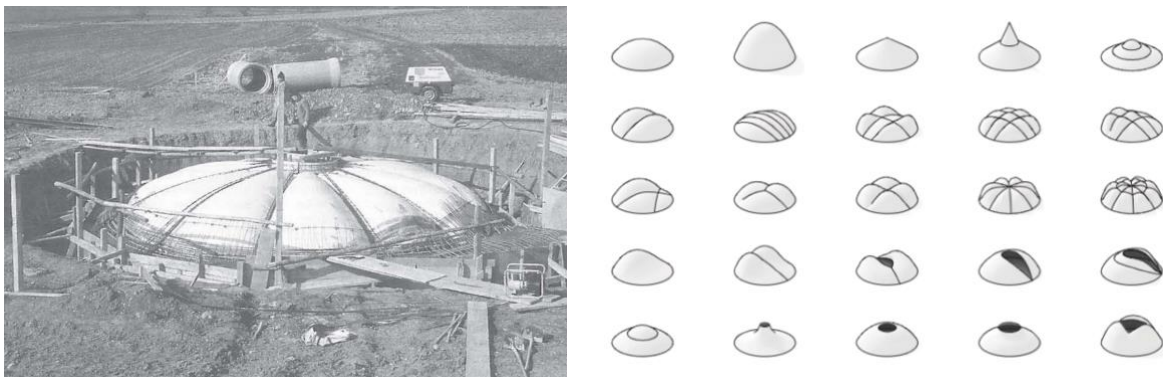


Figure 1: left) Cable-restrained pneumatic formwork for a rainwater interceptor tank [16]; right) A variety of compression-only shell geometries for a circular support that can potentially be built with pneumatics [17].

2. Related work

Inflatable structures fall within the broader category of tensile architectures, distinguished by their reliance on air pressure for form and stability. Throughout history, many researchers have investigated how to understand and determine the principles guiding the shapes and behaviours of such structures.

Early explorations centred around physical testing. In the 1960s, Frei Otto documented a set of experimental pneumatic structures in his book *Tensile Structures, Vol. 1* [18], where he employed cables and meshes to restrain the elastic membrane. Most of these designs were rooted in architectural pragmatism with potential scalability for use as shelters and roofs. More recent experiments include *Inflated Restraint* [11], which uses cables to shape large areas of anticlastic curvature; *Pneulastics* [9], which experiments on the influence of membrane thickness on shape control; and Paul et al.'s development [19] of an interactive design and fabrication procedure that can robotically modulate the membrane by adding constraints.

Advancements in computer technology have given rise to numerous computational methodologies for the form finding of cable nets, prestressed membranes, and pneumatic structures. These approaches can be classified as 1) geometric methods, including the force density method (FDM) [20] and the combinatorial equilibrium modelling method (CEM) [21]; 2) dynamic relaxation methods (DRM) [17]; and 3) finite element method (FEM) [17].

FDM is the state-of-the-art method for form finding tensile structures. It uses a concept known as force density, the ratio of the force within an element to its length, to transform a non-linear array of equilibrium equations into a linear format, providing specified boundary conditions and external loads. Conversely,

CEM constructs equilibrium through sequential steps using 3D graphic statics and allows alterations in topology and the designation of tension and compression members. In [21], CEM was used for the conceptual design of air-supported structures. Despite the geometric foundation of FDM and CEM, they do not account for material properties, and thus, an additional step of materialisation is required. DRM solves dynamic equilibrium by converging towards a steady-state solution [22]. However, these methods are favourable in the case of cable networks, and the translation of axial forces into membrane stresses can pose challenges. While uniform or gradient stress distributions facilitate straightforward materialisation into cutting patterns, non-uniform distributions may induce distortion due to shear stresses [12].

On the contrary, FEM incorporates both the material properties and the geometric configurations. Widely adopted in engineering for structural analysis and direct form finding [23], FEM has also been applied to the inverse design of inflatables, aiming to achieve predefined geometries [24], [25], [26]. Using FEM for inverse design is notably difficult because of the large search space for unknown variables such as undeformed geometry and material characteristics, and the optimisation process is often non-linear and non-convex, posing substantial challenges. Utilising FEM, Disney Research has investigated how to use different patches, as well as elastic membranes, to fit a target geometry [25]. Moreover, FEM-based optimisation demands significant computational resources, particularly when dealing with complex meshes and non-linear material models [26].

3. Methodology

This paper aims to develop a method for restrained pneumatic formwork, which accounts for the first layer of the material's self-weight (e.g. wet concrete) and enables the creation of complex target shapes upon inflation. We propose the workflow illustrated in Figure 2. Given a target geometry and external loads (1), we first solve a best-fit optimisation using the iterative FDM (2) and materialise the force flows (3) by varying the material properties using FEM (4).

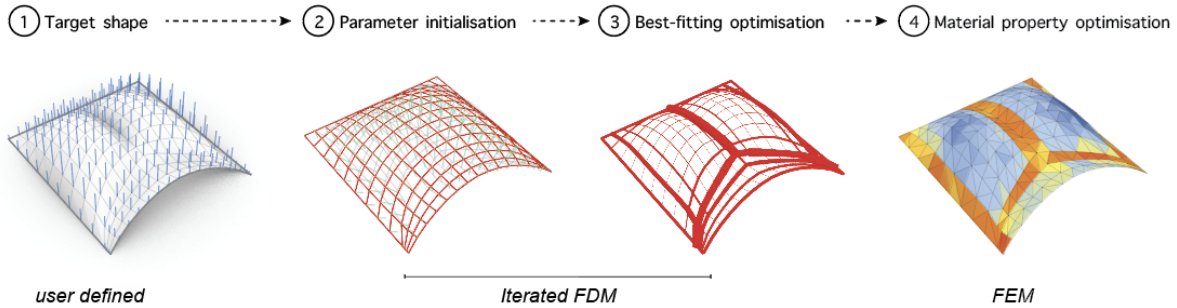


Figure 2: Outline of the workflow for designing the restrained pneumatic formwork.

3.1. Iterative FDM and best-fitting optimisation

In a discrete network, the force density method (FDM) introduces the force density q as the ratio of axial force, F , to its length, l :

$$q = F / l \quad (1)$$

Every free node in the network is in equilibrium under external loads. This can be represented mathematically as:

$$p_x = C_N^T Q C_N x_N + C_N^T Q C_F x_F \quad (2)$$

$$p_y = C_N^T Q C_N y_N + C_N^T Q C_F y_F \quad (3)$$

$$p_z = C_N^T Q C_N z_N + C_N^T Q C_F z_F \quad (4)$$

where p is the external load, C_N is the branch-node connectivity matrix of the free nodes, C_F is the matrix of fixed nodes and Q is the diagonal matrix of the force densities.

By setting $D_N = C_N^T Q C_N$ and $D_F = C_N^T Q C_F$, the free nodal positions can be found:

$$x_N = D_N^{-1}(p_x - D_F x_F) \quad (5)$$

$$y_N = D_N^{-1}(p_y - D_F y_F) \quad (6)$$

$$z_N = D_N^{-1}(p_z - D_F z_F) \quad (7)$$

The equilibrium geometry under air pressure can be found iteratively using FDM. The inflation forces are always pointing outwards and perpendicular to the membrane surface. By starting with an initial geometric configuration, the tributary areas impacted by internal pressure can be calculated as nodal forces. Thus, the form-finding procedure needs to iterate until the disparity between successive equilibrium geometries falls below a predetermined threshold.

Based on the direct form finding, we can optimise the force densities q to find a best-fitting solution for the target geometry. Assuming that the reference compression-only geometry is derived using thrust network analysis (TNA) [27], the same discrete topology can be used for our optimisation (Figure 2-1). The first step involves setting an inflation pressure and initial force densities to reach a first state of equilibrium (Figure 2-2).

We minimise the sum of distance D_i between the nodal position of the free vertices X_i and an approximation of the objective surface S :

$$\min \sum_i D_i^2 \quad (8)$$

Given S_i as the closest point on the reference surface, equation (8) can be written as the following energy function, where x_i , y_i , and z_i are a function of q according to equations (5) (6) (7).

$$f(q) = \sum_i \|X_i - S_i\|^2 \quad (9)$$

To identify the best-fitting solution, we aim to find the optimal q that minimizes the energy function $f(q)$. We employ a gradient descent algorithm, updating the force densities as well as the closest fitting plane in each step as follows:

$$q(t + 1) = q(t) - \lambda \nabla f(q(t)) \quad (10)$$

Here λ is the time step, and ∇ is the gradient operator. Applying the chain rule, the gradient of the energy function can be analytically derived as:

$$\nabla f(q) = \sum_i 2 * (X_i - S_i) \frac{dX_i}{dq} \quad (11)$$

Here, the gradients are:

$$\frac{dx}{dq} = -D_N^{-1} C_N^T \text{diag}(Cx) \quad (12)$$

$$\frac{dy}{dq} = -D_N^{-1} C_N^T \text{diag}(Cy) \quad (13)$$

$$\frac{dz}{dq} = -D_N^{-1} C_N^T \text{diag}(Cz) \quad (14)$$

We implemented this section in Python using numerical computing package NumPy and the COMPAS framework [28].

3.2 Material properties optimisation

In Section 3.1, we ascertain the magnitude of forces within our discrete network, albeit in a manner that is independent of material properties and requires an additional materialisation step. Instead of searching for an ideal undeformed geometry utilising homogeneous materials, we seek to modify the material properties to adjust the stiffness. This modification aims to maintain a uniform deformation ratio across the surface.

The force-density outcomes allow for the calculation of the undeformed edge length l_0 through the equation:

$$l_0 \left(I + \frac{F}{EA} \right) = l \quad (15)$$

Here, E represents Young's modulus along the edge, and A is the cross-sectional area perpendicular to the edge. To maintain uniform deformation $\frac{l_0}{l}$ across the mesh, we keep the ratio $\frac{F}{EA}$ constant.

$$\frac{F}{EA} = c \quad (16)$$

This implies that the modulus E should be directly proportional to the force F , or $E \propto F$. Considering a homogeneous material's thickness allows for the adjustment of E by locally varying the thickness t while maintaining $\frac{F}{tE_0A}$ constant, leading to $t \propto F$.

From equation (15), the undeformed mesh is determined by scaling the target geometry by a factor r .

$$r = \frac{l_0}{l} \quad (17)$$

Parameterising r , t and pressure p within the FEM, we can minimise the deviation from the target surface S . We add the regularisation term L_u to the objective function, which is the thickness Laplacian on the mesh faces to ensure smooth material variation.

$$\min \sum_i ||X_i - S_i||^2 + ||L_u||^2 \quad (18)$$

The nodal positions X_i can be calculated by the principle of virtual work, ensuring equilibrium between membrane stresses S and external loads p , which include the self-weight of the external materials and applied surface pressure over the membrane area A .

$$\delta w = \int_A (tS : \delta E - p \delta u) dA = 0 \quad (19)$$

Here δw represents the virtual work done, δE is the strain tensor, and δu is the virtual displacement.

This section's implementation utilises C++ alongside the Eigen [29] and Geometry Central libraries [30]. We solve the equilibrium equation (19) with a Newton-Raphson method combined with a line search and employ a genetic algorithm for the optimisation problem of equation (18).

4. Results and Discussion

4.1 Results

We test our workflow on a creased vault, taken from [4], which is a synclastic vault form found using TNA and its user interface RhinoVault [5], [27]. During the form finding, we define the topology of the thrust network as well as the magnitude of the gravity load, which will be a 2cm thick light-weight concrete (1600kg/m^3) on the formwork. The vault has geometric features, i.e. creases, that introduce anti-clastic parts into the geometry. Three sides of the boundary are fixed, and one side is open.

In the best-fitting optimisation, the boundary vertices are all fixed, including the ones along the opening. The optimised force densities are depicted in Figure 3, left. We apply the isotropic St. Venant–Kirchhoff material law for the FEM optimisation. The standard membrane has Young's modulus of 50kPa and the Poisson's ratio of 0.38. Figure 3, right, illustrates variations in membrane thickness obtained from the optimisation; we constrain the membrane thickness to range between 0.12 and 1.2 compared to a standard membrane. Controlling and fabricating membranes with variable thickness, however, poses practical challenges. Consequently, based on our findings, we categorise the thickness into three distinct groups and aimed to minimise the deviation from the target geometry. The result with three materials, shown in Figure 4, indicates a maximum deviation of 0.5% in the largest span of the structure compared to the input geometry.

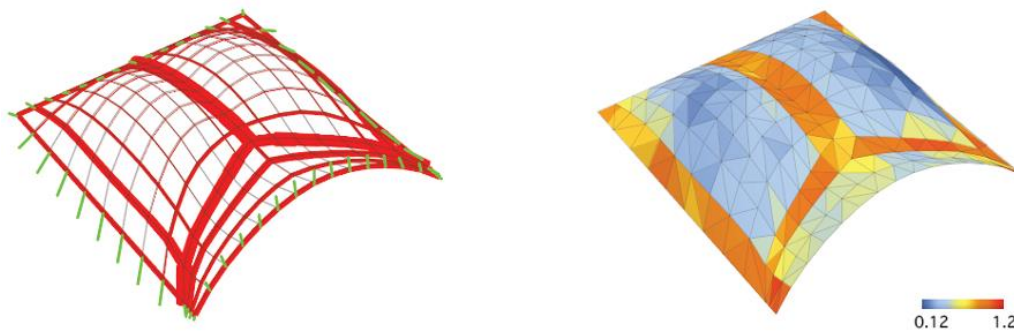


Figure 3: Creased vault: left) Force density results shown in red, and reaction forces shown in green; right) Optimised membrane thickness.

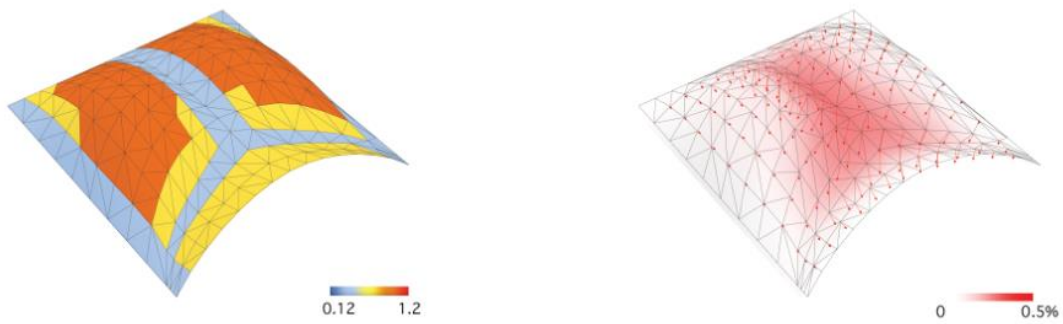


Figure 4: left) Creased vault membrane thickness, limited to only three different membrane thicknesses; right) Deviation from the target geometry.

Additional results are presented in Figures 5 and 6.

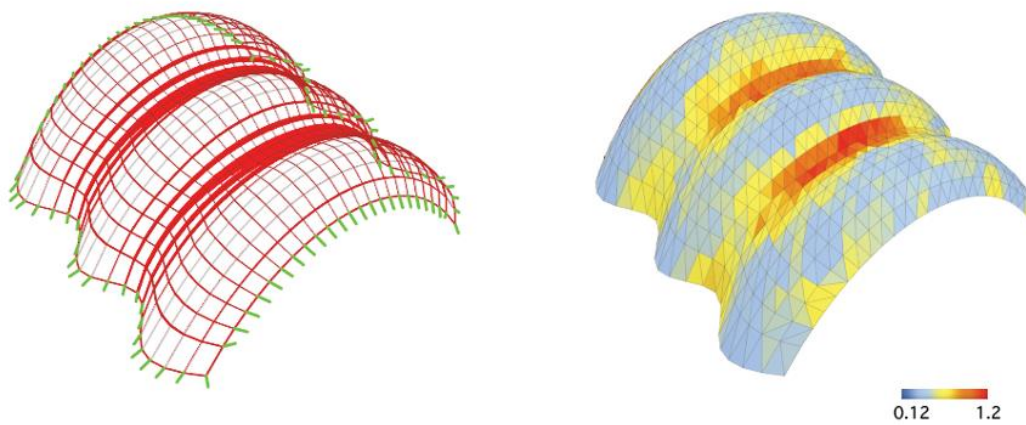


Figure 5: Barrel vault; left) Force density results; right) optimised membrane thickness.

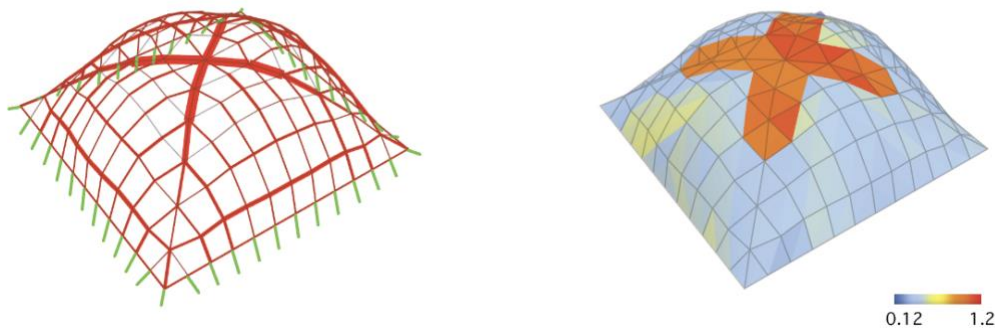


Figure 6: Cross vault; left) Force density results; right) optimised membrane thickness.

4.2 Discussion

Our methodology divides the task of inverse design of the pneumatic structures into a two-part process. The initial phase employs the force density method to determine the force distribution over the surface quickly. Drawing from these results, the choice of material can then be specified, ranging from cable networks, as documented in existing literature [12], [13], to continuous membranes with variable material properties. While the direct optimisation for inverse form finding via FEM is often challenging and not straightforward, the preliminary force density outcomes serve as an effective starting point for the material property optimisation, which then converges quickly. We can also extend our method to design hybrid systems, such as a combination of cables and membranes or bending-active rods and membranes.

Additionally, it is important to note that although this paper's outcome primarily focuses on the use of homogeneous materials, the material model can be adapted in Section 3.2 to accommodate anisotropic materials, such as orthotropic fabrics or knitted fabric with different knitting patterns.

An observation from our study in Section 3.1 indicates that for certain input geometries, such as Figure 6, our method may settle into a local minimum. This is because TNA assumes all vertices are constrained in the xy -direction, and the gravity loads only have a z -component. The presence of non-vertical loads from air pressure invalidates this constraint. In FDM, vertices are free to move, and nodal loads can be applied in any direction. Thus, in such instances, to have a feasible, best-fitting solution for the force densities, we can either remesh the input network topology, or add a subsequential step to identify the nearest face on the mesh and calculate the distance from the point to this plane instead of the corresponding vertices.

However, the scope of this paper does not extend to the practical aspects of fabrication, which remains an area for future investigation.

Acknowledgements

The research is made possible through funding provided by the Architecture & Technology doctoral fellowship of the Institute of Technology in Architecture (ITA) at ETH Zurich. We thank Stephan A. Kollmann for the technical support in C++. The authors declare that there are no conflicts of interest regarding the publication of this paper. The source code is available upon request in the spirit of open science and reproducibility.

References

- [1] R. Verma, "Advancement in Inflatable – 'A Review'".
- [2] J. Cremers, "Environmental Impact of Membrane and Foil Materials and Structures – Status Quo and Future Outlook," p. 13.
- [3] B. Barton, "Recent Work on the Design and Construction of Air Inflated Structures," *Procedia Eng.*, vol. 155, pp. 47–60, 2016, doi: 10.1016/j.proeng.2016.08.006.
- [4] D. Panozzo, P. Block, and O. Sorkine-Hornung, "Designing unreinforced masonry models," *ACM Trans. Graph.*, vol. 32, no. 4, pp. 1–12, Jul. 2013, doi: 10.1145/2461912.2461958.
- [5] M. Rippmann, "Funicular Shell Design: Geometric approaches to form finding and fabrication of discrete funicular structures," 2016. doi: 10.3929/ethz-a-010656780.
- [6] "The Fabric Formwork Book: Methods for Building New Architectural and Structural Forms in Concrete," Routledge & CRC Press. Accessed: Apr. 06, 2023. [Online]. Available: <https://www.routledge.com/The-Fabric-Formwork-Book-Methods-for-Building-New-Architectural-and-Structural/West/p/book/9780415748865>

- [7] W. J. Hawkins *et al.*, “Flexible formwork technologies – a state of the art review,” *Struct. Concr.*, vol. 17, no. 6, pp. 911–935, 2016, doi: 10.1002/suco.201600117.
- [8] D. Bini, “A new pneumatic technique for the construction of thin shells,” presented at the the International Association for Shell Structures. Proceedings for the First IASS International Colloquium on Pneumatic Structures, Germany: University of Stuttgart, May 1967.
- [9] A. Rizou, E. Soriano, and R. Sastre, “PNEULASTICS, pneumatically activated differentiated stretchable membranes,” 2019.
- [10] W. Sobek, “Die Herstellung von Betonschalen auf pneumatisch gestützten Schalungen,” *Concrete shells constructed on air-supported formwork*, 1991, doi: 10.18419/opus-6965.
- [11] P. Ayres, P. Vestartas, and M. Thomsen, “Enlisting Clustering and Graph-Traversal Methods for Cutting Pattern and Net Topology Design in Pneumatic Hybrids,” 2018, pp. 285–294. doi: 10.1007/978-981-10-6611-5_25.
- [12] D. Veenendaal and P. Block, “Design process of prestressed membrane formworks for thin-shell structures,” p. 12, 2015.
- [13] T. V. Mele and P. Block, “A Novel Form Finding Method for Fabric Formwork for Concrete Shells,” 2010.
- [14] C. W. Lin, G. Mattei, I. Cheibas, C. Du, P. Aejmelaeus-Lindström, and F. Gramazio, “PneuPrint: 3D printing on inflatables,” *Archit. Struct. Constr.*, vol. 3, no. 2, pp. 217–234, Jun. 2023, doi: 10.1007/s44150-023-00092-x.
- [15] M. A. Popescu, “KnitCrete: Stay-in-place knitted formworks for complex concrete structures,” PhD Thesis, ETH Zurich, 2019. Accessed: Apr. 03, 2024. [Online]. Available: <https://www.research-collection.ethz.ch/handle/20.500.11850/408640>
- [16] J. Schlaich and W. Sobek, “Suitable shell shapes,” 1986, doi: 10.18419/opus-6988.
- [17] S. Adriaenssens, P. Block, D. Veenendaal, and C. Williams, *Shell Structures for Architecture: Form Finding and Optimization*. Routledge, 2014.
- [18] F. Otto, *Tensile Structures: Vol. 1 : Pneumatic Structures*. 1962.
- [19] P. Poinet, E. Baharlou, T. Schwinn, and A. Menges, *Adaptive Pneumatic Shell Structures: Feedback-driven robotic stiffening of inflated extensible membranes and further rigidification for architectural applications*. 2016. doi: 10.52842/conf.ecaade.2016.1.549.
- [20] H.-J. Schek, “The force density method for form finding and computation of general networks,” *Comput. Methods Appl. Mech. Eng.*, vol. 3, no. 1, pp. 115–134, Jan. 1974, doi: 10.1016/0045-7825(74)90045-0.
- [21] Z. Wan, P. O. Ohlbrock, P. D’Acunto, Z. Cao, F. Fan, and J. Schwartz, “A form-finding approach for the conceptual design of air-supported structures using 3D graphic statics,” *Comput. Struct.*, vol. 243, p. 106401, Jan. 2021, doi: 10.1016/j.compstruc.2020.106401.
- [22] Barnes M R, Wakefield D., “Dynamic relaxation applied to interactive form finding and analysis of air-supported structures,” in *Proceedings of Conference on the Design of Air-supported Structures*, 1984, pp. 147–161.
- [23] Y. Wu *et al.*, *Form-finding and construction of ice composite shell structures*. 2017.

- [24] J. Panetta, F. Isvoranu, T. Chen, E. Siéfert, B. Roman, and M. Pauly, “Computational inverse design of surface-based inflatables,” *ACM Trans. Graph.*, vol. 40, no. 4, p. 40:1-40:14, 2021, doi: 10.1145/3450626.3459789.
- [25] M. Skouras *et al.*, “Designing inflatable structures,” *ACM Trans. Graph.*, vol. 33, no. 4, pp. 1–10, Jul. 2014, doi: 10.1145/2601097.2601166.
- [26] M. Skouras, B. Thomaszewski, B. Bickel, and M. Gross, “Computational Design of Rubber Balloons,” *Comput. Graph. Forum*, vol. 31, no. 2pt4, pp. 835–844, May 2012, doi: 10.1111/j.1467-8659.2012.03064.x.
- [27] P. Block, “Trust Network Analysis : exploring three-dimensional equilibrium,” Nov. 2009.
- [28] “COMPAS.” Accessed: Nov. 30, 2022. [Online]. Available: <https://compas.dev/index.html>
- [29] “Eigen (C++ library).” [Online]. Available: eigen.tuxfamily.org
- [30] “Geometry Central.” [Online]. Available: <https://geometry-central.net/>

Copyright Declaration

Before publication of your paper in the Proceedings of the IASS Annual Symposium 2024, the Editors and the IASS Secretariat must receive a signed Copyright Declaration. The completed and signed declaration may be uploaded to the EasyChair submission platform or sent as an e-mail attachment to the symposium secretariat (papers@iass2024.org). A scan into a .pdf file of the signed declaration is acceptable in lieu of the signed original. In the case of a contribution by multiple authors, either the corresponding author or an author who has the authority to represent all the other authors should provide his or her address, phone and E-mail and sign the declaration.

Paper Title: __ Design of restrained pneumatic formwork – Inverse form finding and materialisation for free form geometries

Author(s): __ Chaoyu DU, Ziqi WANG, Tom VAN MELE, Philippe BLOCK

Affiliation(s): __ Block Research Group, ETH Zurich

Address: __ Stefano-Franscini-Platz 1, 8093, 8049

Phone: __+41 765873898

E-mail: __chaoyu.du@arch.ethz.ch


I hereby license the International Association for Shell and Spatial Structures to publish this work and to use it for all current and future print and electronic issues of the Proceedings of the IASS Annual Symposia. I understand this licence does not restrict any of the authors' future use or reproduction of the contents of this work. I also understand that the first-page footer of the manuscript is to bear the appropriately completed notation:

Copyright © 2024 by <name(s) of all of the author(s)>

Published by the International Association for Shell and Spatial Structures (IASS) with permission

If the contribution contains materials bearing a copyright by others, I further affirm that (1) the authors have secured and retained formal permission to reproduce such materials, and (2) any and all such materials are properly acknowledged by reference citations and/or with credits in the captions of photos/figures/tables.

Printed name: __Chaoyu Du

Signature: __ 

Location: __Zurich

Date: __28 Jun 2024